

Hyperbolic Fractional Chern insulators

Ai-Lei He,^{1,*} Lu Qi,¹ Yongjun Liu,^{1,†} and Yi-Fei Wang^{2,3}

¹College of Physics Science and Technology, Yangzhou University, Yangzhou 225002, China

²Zhejiang Institute of Photoelectronics & Zhejiang Institute for Advanced Light Source, Zhejiang Normal University, Jinhua 321004, China

³Center for Statistical and Theoretical Condensed Matter Physics, and Department of Physics, Zhejiang Normal University, Jinhua 321004, China

(Dated: July 9, 2024)

Fractional Chern insulators (FCIs) have attracted intensive attention for the realization of fractional quantum Hall states in the absence of an external magnetic field. Most of FCIs have been proposed on two-dimensional (2D) Euclidean lattice models with various boundary conditions. In this work, we investigate hyperbolic FCIs which are constructed in hyperbolic geometry with constant negative curvature. Through the studies on hyperbolic analogs of kagome lattices with hard-core bosons loaded into topological flat bands, we find convincing numerical evidences of two types of $\nu = 1/2$ FCI states, *i.e.*, the conventional and unconventional FCIs. Multiple branches of edge excitations and geometry-dependent wave functions for both conventional and unconventional $\nu = 1/2$ FCI states are revealed, however, the geometric degree of freedom in these FCIs plays various roles. Additionally, a center-localized orbital plays a crucial role in the unconventional FCI state.

Introduction.—Fractional Chern insulators (FCIs) [1–22], which realize fractional quantum Hall states without an external magnetic field, have been theoretically proposed for more than a decade. Most recently, there are significantly experimental advances in the realization of FCIs in Moiré superlattice systems [23–27]. To achieve FCI states, topological flat band (TFB) models are required because TFBs can quench kinetic energy and enhance interaction effectively, which is in analogy of Landau levels (LLs) [1–5, 20–22]. By tuning hopping parameters of Chern insulator (CI) models, a series of TFB models have been proposed [28–35]. Due to the similarity between TFBs and LLs, one can define the mapping relationship between single-particle states in CIs and LL wave functions (WFs) in quantum Hall states [6]. Subsequently, several trial WFs for FCIs can be explicitly constructed in Euclidean lattices with various boundary conditions [6, 10, 14, 36]. Inspired by the analytic expression of Laughlin WFs [37] and the generalized Pauli principle (GPP) [38–40], some of us have proposed a direct and effective approach to construct FCI states in disk geometry [41, 42] based on the Jack polynomials (Jacks) [43–45] and single-particle states of TFBs. Trial WFs for FCIs in singular CI models have been constructed directly [46, 47] as well and the inherent geometric factor for FCIs have been revealed [46]. Different from CIs in disk geometry, a defect-core state emerges in singular CI models. Intriguingly, the defect-core orbital in the TFB models can lead to multiple branches of edge excitations (EEs) and two types of $\nu = 1/2$ FCIs in which the geometry plays the same role [47].

Unlike singular surfaces with a point of singular curvature in real space, two-dimensional (2D) hyperbolic geometry has constant negative curvature, but without point singularities. As a new class of 2D lattice structures, hyperbolic lattice models constructed in the

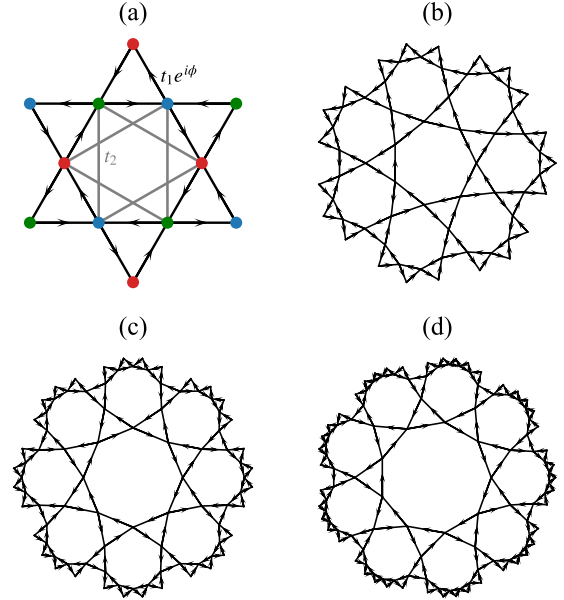


FIG. 1. (color online). Kagome and kagomelike lattice models. (a) Euclidean kagome lattice model host three atoms in a unit cell which are colored with red, blue and green, respectively. To obtain a nearly TFB, we introduce the NN hopping with staggered magnetic fluxes ($t_1 e^{i\phi}$) and the NNN hopping t_2 . We can introduce the staggered magnetic fluxes in (b) the HKG, (c) the OKG and (d) the NKG lattices. The phase difference are represented by the arrows and these hyperbolic lattices are represented in the Poincaré-disk model.

hyperbolic plane host several exotic physics phenomena which is beyond in 2D Euclidean lattice models, such as hyperbolic band theory and crystallography [48–52], generalized Bloch theory and non-Abelian Bloch states [51, 53, 54], periodic boundary conditions and thermodynamic limit [55–57], unusual flat band [58, 59] and TFBs [60, 61], large disorder critical strengths in

Anderson localization [62, 63], effects of strong correlations [64–66], Hofstadter spectra [52, 67–69] and topological states [68, 70–78], non-Hermitian effect [79], holographic duality [80], etc. Experimentally, 2D hyperbolic lattice structures have been realized in circuit quantum electrodynamics (cQED) [50, 81] and classical electric-circuit networks [60, 71, 73, 75, 82, 83]. Recent theoretical and experimental advances have stimulated interest in the study of condensed matter systems in hyperbolic lattice models. And a very challenging topic is whether the existence of FCIs in hyperbolic lattices and how to characterize them.

In this work, we explicitly demonstrate the existence of two types of $\nu = 1/2$ bosonic FCI states in hyperbolic analogs of kagome lattice models based on the exact diagonalization (ED) results, *i.e.*, the conventional and unconventional FCIs. These two types of FCIs can be characterized based on the EEs and trial WFs for the ground state (GS). According to the exact numerical results, we find more than one branches of EEs and the geometry-dependent GS WFs for these $\nu = 1/2$ bosonic FCIs. Different from the conventional FCI state, the unconventional FCI state depends on the low-energy center-localized orbital created by the geometry of hyperbolic lattices. With the aid of trial WFs, we find the geometry of hyperbolic lattices plays different roles in these two types of FCIs, in sharp contrast to $\nu = 1/2$ FCIs in singular lattices [47].

Models and topological flat bands.— The Euclidean kagome lattice model consists of triangles and hexagons [as illustrated in Fig. 1 (a)]. This kagome lattice model hosts a TFB with flatness ratio about 20 [33] where the nearest-neighbor (NN) hopping with staggered magnetic fluxes and the next-nearest-neighbor (NNN) hopping are considered. The NN and NNN hopping terms are respectively $t_1 e^{i\phi}$ and t_2 , where ϕ stems from the staggered magnetic fluxes. In this work, we consider three hyperbolic analogs of kagome lattice models, *i.e.*, kagome models made with heptagons, octagons, and nonagons, which are referred to as the heptagon-kagome (HKG), the octagon-kagome (OKG) and the nonagon-kagome (NKG) lattices, respectively. And these hyperbolic lattices are represented using the Poincaré-disk model [in Fig. 1 (b)-(d)]. To obtain TFBs in these kagome-like lattice models, we consider NN and NNN hopping processes similar to the Euclidean kagome TFB model [33]. For the present models, each NN bond carries the phase $\pm\phi$, and the signs of these phases are represented by the directions of arrows [shown in Fig. 1 (b)-(d)]. One can easily verify the total flux of each hyperbolic kagome lattice model is vanished. The tight-binding Hamiltonian of these hyper-

bolic lattice models can be written as

$$H = t_1 \sum_{\langle \mathbf{r}\mathbf{r}' \rangle} \left[e^{i\phi_{\mathbf{r}'\mathbf{r}}} a_{\mathbf{r}'}^\dagger a_{\mathbf{r}} + \text{H.c.} \right] + t_2 \sum_{\langle\langle \mathbf{r}\mathbf{r}' \rangle\rangle} \left[a_{\mathbf{r}'}^\dagger a_{\mathbf{r}} + \text{H.c.} \right], \quad (1)$$

where $a_{\mathbf{r}}^\dagger$ ($a_{\mathbf{r}}$) creates (annihilates) a particle at site \mathbf{r} . $\langle \dots \rangle$ and $\langle\langle \dots \rangle\rangle$ denote the NN and NNN pairs of sites and their corresponding hopping integrals are t_1 and t_2 . $\phi_{\mathbf{r}'\mathbf{r}} = \pm\phi$ is the phase difference between the NN sites.

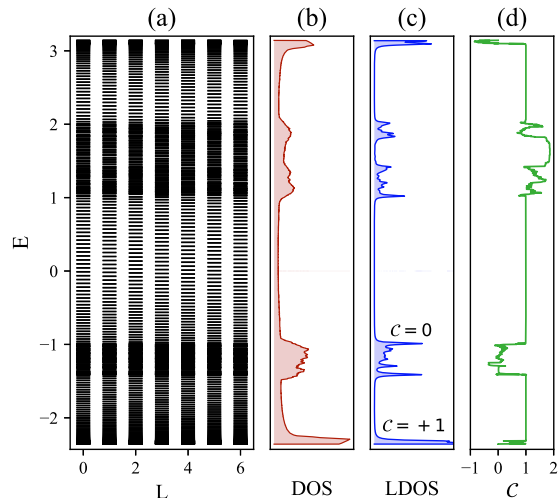


FIG. 2. (color online). Topological flat “band” of the HKG lattice model. (a) Energy spectrum of HKG lattice model are arranged in various angular momentum L sectors. (b) the density of states (DOS), (c) the local density of states (LDOS) in the bulk and (d) the real-space Chern number for this energy spectrum. Here, we consider a 2072-site HKG model and the hopping parameters are $t_1 = -1.0$, $t_2 = 0.19$ and $\phi = -0.22\pi$.

Both these hyperbolic kagome lattice models and their corresponding Hamiltonian [Eq. (1)] respectively hosts sevenfold, eightfold and ninefold rotational symmetries. One can obtain single-particle energy spectra arranged in various angular momentum sectors because the angular momentum is a good quantum number. To obtain nearly TFBs in the kagome-like lattice models, we adopt the TFB parameters of Euclidean kagome lattice model [33], *i.e.*, $t_1 = -1.0$, $t_2 = 0.19$ and $\phi = -0.22\pi$. Here, we take the HKG model as an example and OKG, NKG lattice models host similar properties [see S1 in the Supplemental Material (SM) [84]]. The single-particle energy states of the HKG model with open boundary condition is obtained by diagonalizing the Hamiltonian [Eq. (1)] classified with the quantum number of angular momentum $L = 0, 1, 2, 3, \dots \bmod 7$ [displayed in Fig. 2(a)]. To characterize features of this energy spectrum, the density of states (DOS), local density of states (LDOS) in the bulk and real-space Chern number are respectively considered

in Fig. 2(b)-(d). Based on the DOS and bulk LDOS [see Fig. 2(b)-(c)], the lowest energy bands seems nearly flat and it has a non-zero real-space Chern number, *i.e.*, $\mathcal{C} = +1$. Consequently, we obtain a TFB in the HKG model. However, this TFB may differ from TFBs in Euclidean lattice models, because the lowest energy bands of hyperbolic CI models comprise more than one bands with periodic boundary condition on the basis of the hyperbolic band theory and crystallography [48–52]. The present TFB actually hosts several flat bands with the total Chern number $\mathcal{C} = 1$ [60, 61].

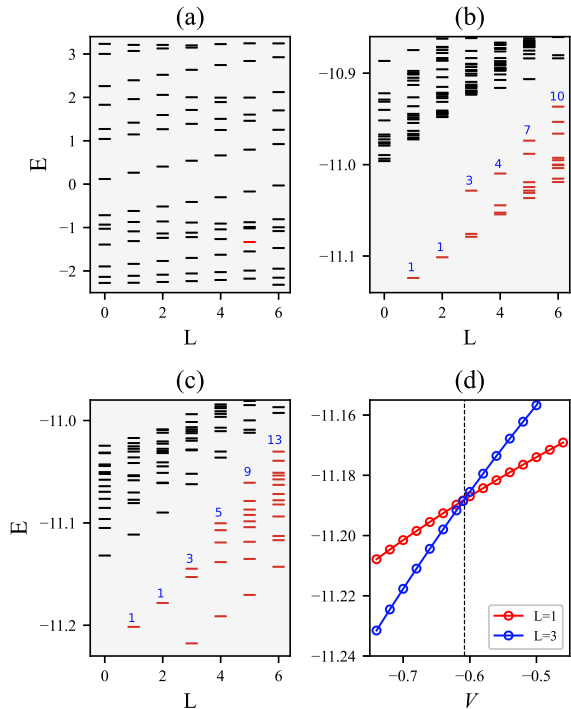


FIG. 3. (color online). (a) Single-particle energy spectrum of the TFB model in a 98-site HKG lattice. One center-localized state near the lowest band is colored with red. (b) EEs for the conventional $\nu = 1/2$ FCIs in the HKG TFB models filling with five hard-core bosons. (c) EEs for the unconventional $\nu = 1/2$ FCIs in the HKG TFB models filling with five hard-core bosons. (d) GS energy for $\nu = 1/2$ FCIs filling with 5 bosons by tuning the NN interaction potential V in HKG TFB model and the crossing point ($V \approx -0.61$) is marked by a black dashed line. L is the angular momentum related to the rotational symmetry. The trap potential is $V_{\text{trap}} = 0.005$.

Edge excitations.—In order to confine the FCI droplet and make the edge modes propagate around the boundary, an additional trap potential is required on the finite-size hyperbolic disks. Here, we choose the harmonic trap with the form $V = V_{\text{trap}} \sum_{\mathbf{r}} |\mathbf{r}|^2 n_{\mathbf{r}}$ [16, 41, 42, 46, 47, 85], where V_{trap} is the trap potential strength and $n_{\mathbf{r}}$ is the number of particles. $|\mathbf{r}|$ is the radius from the disk center. The hyperbolic distance between two points z, z' ($z = x + iy$ as the complex coordinate in the Poincaré

disk) is defined as

$$d(z, z') = \kappa \text{arcosh} \left(1 + \frac{2|z - z'|^2}{(1 - |z|^2)(1 - |z'|^2)} \right), \quad (2)$$

where κ is related to the corresponding negative curvature K , *i.e.*, $\kappa = \sqrt{-K}$ and we set $\kappa = 1$. Accordingly, $|\mathbf{r}| = \text{arcosh}((1 + |z|^2)/(1 - |z|^2))$. The single-particle spectrum of a 98-site HKG model with trap potential $V_{\text{trap}} = 0.02$ is shown in Fig. 3 (a) and the angular momentum of GS is six. Different from single-particle spectrum in 2D Euclidean model, a center-localized state appears near the low-energy band with angular momentum five and the corresponding state is localized around the center of hyperbolic disk [details shown in Fig. 3 (a) and section S2 in the SM [84]]. The center-localized state also appears in the OKG and NKG TFB models (sections S3 and S4 in the SM [84]).

We present the EE spectra for FCIs in the HKG TFB models filling with five hard-core bosons. When considering particles without NN interaction, the total angular momentum of the GS is one and there is a branch of EEs with degeneracy sequences “1,1,3,4,7,10, ...” according to the ED results [as shown in Fig. 3 (b)]. Although the degeneracy sequences of the EEs are not “1,1,2,3,5,7, ...”, this FCI state seems to be a $\nu = 1/2$ FCI for two reasons: i) the total angular momentum of $\nu = 1/2$ FCI GS is $(6 + 1 + 3 + 5 + 0) \bmod 7 = 1$ (the corresponding root configuration $|10101010\rangle_{\text{FCI}}$ and the occupying configuration shown in S2 in the SM [84]); ii) two branches of EEs mix together, and the degeneracy sequences of one branch is “1,1,2,3,5,7, ...” and the other is “0,0,1,1,2,3, ...”, which is reminiscent of FCIs in singular lattices where defect-core orbital leads to multiple branches of EEs [46, 47]. The emergence of two branches of the present FCI may be related to the center-localized orbital.

For the FCIs in singular lattices, energy crossing occurs between the GS and the first excited state by tuning the NN interaction and a FCI state with one particle occupied the defect-core orbital appears with attractive interaction [47]. Inspired by this, we add the NN attractive interaction (we choose $V = -0.7$) in the HKG TFB model. Based on the ED results, we obtain a many-body state whose degeneracy sequences of the EEs become “1,1,3,5,9,13, ...” and the GS angular momentum is three [as illustrated in Fig. 3 (c)]. This state possibly belongs to a $\nu = 1/2$ FCI in which one hard-core boson fills into the center-localized orbital, namely, the unconventional $\nu = 1/2$ FCI. The corresponding root configuration may be $|\underline{1}0101010\rangle_{\text{FCI}}$ (the occupying configuration in S2 in the SM [84]), where $\underline{1}$ denotes one particle occupying the center-localized orbital, and the total angular momentum is $(5 + 0 + 2 + 4 + 6) \bmod 7 = 3$ consistent with the numerical results. Multiple branches of EEs mix together as well and each branch hosts the degeneracy sequences

“1,1,2,3,5,7, ...”, (*i.e.* “1,1,2,3,5,7, ...” + “0,0,1,1,2,3, ...” + “0,0,0,1,1,2, ...” + “0,0,0,0,1, ...”). By tuning the NN interaction potential V , energy crossing occurs between the GS and the first excited state [displayed in Fig. 3 (d)], similar to the FCIs in singular lattices [47]. Similar results appear in the OKG and NKG TFB models as well (details shown in S3 and S4 in the SM [84]). However, whether the geometry in these hyperbolic TFB models plays a role and whether it plays the same role for the conventional and unconventional $\nu = 1/2$ FCIs remains unclear.

Trial wave functions.—Based on the GPP, the Jacks and single-particle states of TFBs ($\{|\phi_i\rangle\}$), trial WFs for the $\nu = 1/m$ FCI in disk or singular geometries can be directly constructed with a general expression, *i.e.* $\Psi_{\text{FCI}}^{\nu=1/m} = \sum_l J_{\lambda_l} \Phi_{\lambda_l}^{\text{TFB}}$ [41, 46, 84], where $\Phi_{\lambda_l}^{\text{TFB}}$ is the antisymmetric Slater determinant (for fermions) or symmetric polynomial (for bosons) composed by the single-particle states of TFBs and J_{λ_l} is the expansion coefficients which are related to the l -th basis configurations λ_l which comes from squeezing the root configuration [43–45]. Here we take $\nu = 1/2$ bosonic FCI filling with three bosons as an example. The root configuration is $\Phi_{[4,2,0]}^{\text{TFB}} = |101010\rangle_{\text{TFB}}$ [86], a symmetric polynomial composed of $|\phi_0\rangle$, $|\phi_2\rangle$ and $|\phi_4\rangle$. Based on the squeezing rules [43–45], other basis configurations are obtained, *i.e.*, $\Phi_{[4,1,1]}^{\text{TFB}} = |020010\rangle_{\text{TFB}}$, $\Phi_{[3,2,1]}^{\text{TFB}} = |011100\rangle_{\text{TFB}}$, $\Phi_{[3,3,0]}^{\text{TFB}} = |100200\rangle_{\text{TFB}}$ and $\Phi_{[2,2,2]}^{\text{TFB}} = |003000\rangle_{\text{TFB}}$. Accordingly, the GS of $\nu = 1/2$ FCI can be directly written as $\Psi_{\text{FCI}}^{\nu=1/2} = J_{[4,2,0]} \Phi_{[4,2,0]}^{\text{TFB}} + J_{[4,1,1]} \Phi_{[4,1,1]}^{\text{TFB}} + J_{[3,2,1]} \Phi_{[3,2,1]}^{\text{TFB}} + J_{[3,3,0]} \Phi_{[3,3,0]}^{\text{TFB}} + J_{[2,2,2]} \Phi_{[2,2,2]}^{\text{TFB}}$. For various geometries of lattice systems, the geometric factor β is implicit in the expansion coefficients, $J_{\lambda_l} \equiv J_{\lambda_l}(\beta)$. For example, the geometric factor $\beta = 6/n$ is related to the n -fold rotational symmetry in singular Kagome lattices and the FCI states are dependent on the geometric factor [46, 47].

Inspired by the trial WFs for FCIs in singular Kagome lattices, the trial WFs for $\nu = 1/2$ FCI in HKG lattice (with sevenfold rotational symmetry, *i.e.*, $n = 7$) can be written as $\Psi_{\text{FCI}}^{\nu=1/m} = \sum_l J_{\lambda_l}(f(\beta = 6/7)) \Phi_{\lambda_l}^{\text{TFB}}$ where $f(\beta)$ is a function which is related to the geometric factor β . To obtain the expression of $f(\beta)$, a series of trial WFs for the $\nu = 1/2$ FCI by tuning $f(\beta)$ from 0.1 to 1.5 are constructed. When $f(\beta = 6/7) \approx 0.74$, the WF overlap value (*i.e.*, $\mathcal{O} = |\langle \Psi_{\text{FCI}}^{\nu=1/2} | \Psi_{\text{ED}} \rangle|$), the inner product of trial WF and WF from ED result) is very close to the maximum [details shown in Fig. 4 (a)]. For the conventional $\nu = 1/2$ FCI state in the OKG and NKG TFB models, when the geometric functions are respectively $f(\beta = 6/8) \approx 0.41$ and $f(\beta = 6/9) \approx 0.20$, the corresponding WF overlaps are close to the maximum (details in S6 in the SM [84]). Based on these numerical results, a fitting function is roughly obtained $f_{\text{F}}(\beta = 6/n) = \beta^{6/\beta-5} = (6/n)^{n-5}$ for the conventional

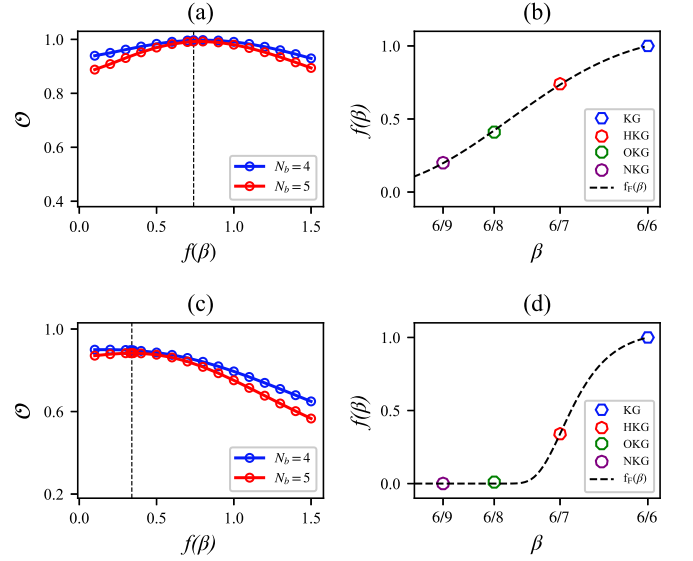


FIG. 4. (color online). (a) WF Overlap between the trial GS WFs and the ED results with variable geometric function $f(\beta)$ for $\nu = 1/2$ FCI filling with $N_b = 4$ and $N_b = 5$ hard-core bosons in HKG TFB models. (b) Based on the WF Overlaps, the suitable geometric function $f(\beta)$ can be verified for $\nu = 1/2$ FCIs in the Euclidean kagome (KG), HKG, OKG and NKG TFB models, and the fitting function $f_{\text{F}}(\beta)$ is obtained. (c) WF Overlap for unconventional $\nu = 1/2$ FCI filling with $N_b = 4$ and $N_b = 5$ hard-core bosons in HKG TFB models. (d) The suitable geometric function $f(\beta)$ for unconventional $\nu = 1/2$ FCIs in hyperbolic lattices and the fitting function $f_{\text{F}}(\beta)$ are obtained.

$\nu = 1/2$ FCI in hyperbolic lattices with n -fold rotational symmetry [in Fig. 4 (b)].

We next consider the unconventional $\nu = 1/2$ FCI where one hard-core boson fills into the center-localized orbital. To obtain this FCI, an attractive interaction $V = -0.7$ is added for the HKG model. Based on the GPP, the Jacks and the center-localized orbital, we construct a series of trial WFs for this $\nu = 1/2$ FCI by tuning $f(\beta)$ from 0.1 to 1.5. The WF overlap values are shown in Fig. 4 (c) and the geometric function is about 0.34 (*i.e.*, $f(\beta = 6/7) \approx 0.34$) in terms of the max overlap value. The max WF overlap values is not very high (~ 0.897 for four bosons and ~ 0.883 for five bosons), because the occupied center-localized orbital [colored with red in Fig. 3 (a)] is far from the TFB orbitals and even near the high-energy bulk orbital. Trial WFs for this unconventional $\nu = 1/2$ FCI in the OKG and NKG TFB models are constructed as well and their corresponding geometric functions are close to zero (see S6 in the SM [84]). A possible fitting function for the geometric function can be roughly obtained $f_{\text{F}}(\beta = 6/n) = \beta^{6/\beta} (6/\beta)^{-(6/\beta-6)} = (6/n)^{n(n-6)}$ [in Fig. 4 (d)]. Though these geometric functions may be not absolutely in accord with the ED WFs, one can clearly find for the conventional and unconventional $\nu = 1/2$ FCIs, geometry of hyperbolic lattices plays different roles,

in stark contrast to FCIs in singular lattices in which the geometry plays the same role [47].

Summary and discussion.—We explicitly investigate $\nu = 1/2$ FCIs in hyperbolic TFB models filling with hard-core bosons, and the conventional and unconventional FCIs emerge. These two types of FCIs can be identified on the basis of the EEs and trial WFs. According to the ED results, these FCIs host more than one branches of EEs and the degeneracy sequence of each branch is “1, 1, 2, 3, 5 ...”, which can reveal the characterisation of $\nu = 1/2$ FCIs. Based on the GPP, the Jacks and single-particle states, we construct a series of trial WFs and the high WF overlap values manifest that for the conventional FCI state, all particles occupy the TFB orbitals, however, for the unconventional FCI state, one particle occupies the center-localized orbital. More intriguingly, we find these FCIs are related to the geometry of hyperbolic lattices and the geometry plays various roles in the conventional and the unconventional FCIs. It will be a challenging but significant issue to explore the reason why the geometry plays various roles in future studies.

Our findings might open up several future directions on hyperbolic FCIs. The center-localized orbital plays a crucial role in the realization of unconventional FCIs. Why does the center-localized state appear in hyperbolic lattices and what is the relationship between the center-localized state and non-Abelian Bloch states [51, 53, 54]? Geometry responses (such as the gravitational anomaly and electromagnetic response) have been revealed in the curved fractional quantum Hall states [87–94]. It is very interesting to explore geometry responses in hyperbolic FCIs as well. Additionally, non-Abelian FCIs have already been systematically studied in 2D Euclidean lattices [8, 18, 20, 21, 42], while non-Abelian FCIs in hyperbolic lattices await to be explored. FCIs have been verily observed in Moiré systems [23–27]. The study of electronic properties and flat bands in possible hyperbolic Moiré systems will also be appealing. Experimentally, the realization of 2D hyperbolic lattices have been reported in both the cQED [50, 81] and classical electric-circuit networks [60, 71, 73, 75, 82, 83]. Recently, the TFBs in OKG model have been realized in the electric circuits [60], however, it is very difficult to add interactions in the electric circuits. The cQED [50, 81] and cold-atomic systems can be candidates to realize hyperbolic FCIs in which both TFBs and interactions are possibly achieved.

Acknowledgments— This work was supported in part by the NSFC under Grants Nos. 12204404 (A.-L.H.), 12304557 (L.Q.) and 11874325 (Y.-F.W.), and the Natural Science Foundation of Jiangsu Higher Education Institutions of China, Grant No. 22KJB140019 (A.-L.H.).

* healei@yzu.edu.cn

† yjliu@yzu.edu.cn

- [1] T. Neupert, L. Santos, C. Chamon, and C. Mudry, *Phys. Rev. Lett.* **106**, 236804 (2011).
- [2] E. Tang, J.-W. Mei, and X.-G. Wen, *Phys. Rev. Lett.* **106**, 236802 (2011).
- [3] D. N. Sheng, Z.-C. Gu, K. Sun, and L. Sheng, *Nature Communications* **2**, 389 EP (2011), article.
- [4] Y.-F. Wang, Z.-C. Gu, C.-D. Gong, and D. N. Sheng, *Phys. Rev. Lett.* **107**, 146803 (2011).
- [5] N. Regnault and B. A. Bernevig, *Phys. Rev. X* **1**, 021014 (2011).
- [6] X.-L. Qi, *Phys. Rev. Lett.* **107**, 126803 (2011).
- [7] B. A. Bernevig and N. Regnault, *Phys. Rev. B* **85**, 075128 (2012).
- [8] Y.-F. Wang, H. Yao, Z.-C. Gu, C.-D. Gong, and D. N. Sheng, *Phys. Rev. Lett.* **108**, 126805 (2012).
- [9] S. A. Parameswaran, R. Roy, and S. L. Sondhi, *Phys. Rev. B* **85**, 241308 (2012).
- [10] Y.-L. Wu, N. Regnault, and B. A. Bernevig, *Phys. Rev. B* **86**, 085129 (2012).
- [11] Y.-F. Wang, H. Yao, C.-D. Gong, and D. N. Sheng, *Phys. Rev. B* **86**, 201101 (2012).
- [12] Z. Liu, E. J. Bergholtz, H. Fan, and A. M. Läuchli, *Phys. Rev. Lett.* **109**, 186805 (2012).
- [13] T. Scaffidi and G. Möller, *Phys. Rev. Lett.* **109**, 246805 (2012).
- [14] Y.-L. Wu, N. Regnault, and B. A. Bernevig, *Phys. Rev. Lett.* **110**, 106802 (2013).
- [15] C. H. Lee, R. Thomale, and X.-L. Qi, *Phys. Rev. B* **88**, 035101 (2013).
- [16] W.-W. Luo, W.-C. Chen, Y.-F. Wang, and C.-D. Gong, *Phys. Rev. B* **88**, 161109 (2013).
- [17] Z. Liu, D. L. Kovrizhin, and E. J. Bergholtz, *Phys. Rev. B* **88**, 081106 (2013).
- [18] Z. Liu, E. J. Bergholtz, and E. Kapit, *Phys. Rev. B* **88**, 205101 (2013).
- [19] M. Claassen, C. H. Lee, R. Thomale, X.-L. Qi, and T. P. Devereaux, *Phys. Rev. Lett.* **114**, 236802 (2015).
- [20] S. A. Parameswaran, R. Roy, and S. L. Sondhi, *Comptes Rendus Physique* **14**, 816 (2013).
- [21] E. J. Bergholtz and Z. Liu, *International Journal of Modern Physics B* **27**, 1330017 (2013).
- [22] Z. Liu and E. J. Bergholtz, in *Reference Module in Materials Science and Materials Engineering* (Elsevier, 2023).
- [23] J. Cai, E. Anderson, C. Wang, X. Zhang, X. Liu, W. Holtzmann, Y. Zhang, F. Fan, T. Taniguchi, K. Watanabe, Y. Ran, T. Cao, L. Fu, D. Xiao, W. Yao, and X. Xu, *Nature* **622**, 63 (2023).
- [24] Y. Zeng, Z. Xia, K. Kang, J. Zhu, P. Knüppel, C. Vaswani, K. Watanabe, T. Taniguchi, K. F. Mak, and J. Shan, *Nature* **622**, 69 (2023).
- [25] H. Park, J. Cai, E. Anderson, Y. Zhang, J. Zhu, X. Liu, C. Wang, W. Holtzmann, C. Hu, Z. Liu, T. Taniguchi, K. Watanabe, J.-H. Chu, T. Cao, L. Fu, W. Yao, C.-Z. Chang, D. Cobden, D. Xiao, and X. Xu, *Nature* **622**, 74 (2023).
- [26] F. Xu, Z. Sun, T. Jia, C. Liu, C. Xu, C. Li, Y. Gu, K. Watanabe, T. Taniguchi, B. Tong, J. Jia, Z. Shi, S. Jiang, Y. Zhang, X. Liu, and T. Li, *Phys. Rev. X* **13**, 031037 (2023).

- [27] Z. Lu, T. Han, Y. Yao, A. P. Reddy, J. Yang, J. Seo, K. Watanabe, T. Taniguchi, L. Fu, and L. Ju, *Nature* **626**, 759 (2024).
- [28] K. Sun, Z. Gu, H. Katsura, and S. Das Sarma, *Phys. Rev. Lett.* **106**, 236803 (2011).
- [29] E. Kapit and E. Mueller, *Phys. Rev. Lett.* **105**, 215303 (2010).
- [30] X. Hu, M. Kargarian, and G. A. Fiete, *Phys. Rev. B* **84**, 155116 (2011).
- [31] W.-C. Chen, R. Liu, Y.-F. Wang, and C.-D. Gong, *Phys. Rev. B* **86**, 085311 (2012).
- [32] F. Wang and Y. Ran, *Phys. Rev. B* **84**, 241103 (2011).
- [33] R. Liu, W.-C. Chen, Y.-F. Wang, and C.-D. Gong, *Journal of Physics: Condensed Matter* **24**, 305602 (2012).
- [34] X.-P. Liu, W.-C. Chen, Y.-F. Wang, and C.-D. Gong, *Journal of Physics: Condensed Matter* **25**, 305602 (2013).
- [35] Z.-Y. Lan, A.-L. He, and Y.-F. Wang, *Phys. Rev. B* **107**, 235116 (2023).
- [36] Y. Zhang and J. Shi, *Phys. Rev. B* **93**, 165129 (2016).
- [37] R. B. Laughlin, *Phys. Rev. Lett.* **50**, 1395 (1983).
- [38] F. D. M. Haldane, *Phys. Rev. Lett.* **67**, 937 (1991).
- [39] Y.-S. Wu, *Phys. Rev. Lett.* **73**, 922 (1994).
- [40] E. J. Bergholtz and A. Karlhede, *Phys. Rev. B* **77**, 155308 (2008).
- [41] A.-L. He, W.-W. Luo, Y.-F. Wang, and C.-D. Gong, *New Journal of Physics* **17**, 125005 (2015).
- [42] A.-L. He, W.-W. Luo, H. Yao, and Y.-F. Wang, *Phys. Rev. B* **101**, 165127 (2020).
- [43] B. A. Bernevig and F. D. M. Haldane, *Phys. Rev. Lett.* **100**, 246802 (2008).
- [44] B. A. Bernevig and F. D. M. Haldane, *Phys. Rev. Lett.* **101**, 246806 (2008).
- [45] B. A. Bernevig and N. Regnault, *Phys. Rev. Lett.* **103**, 206801 (2009).
- [46] A.-L. He, W.-W. Luo, Y.-F. Wang, and C.-D. Gong, *Phys. Rev. B* **99**, 165105 (2019).
- [47] A.-L. He, *Phys. Rev. B* **103**, 115138 (2021).
- [48] J. Maciejko and S. Rayan, *Science Advances* **7**, eabe9170 (2021), <https://www.science.org/doi/pdf/10.1126/sciadv.abe9170>.
- [49] J. Maciejko and S. Rayan, *Proceedings of the National Academy of Sciences* **119**, e2116869119 (2022), <https://www.pnas.org/doi/pdf/10.1073/pnas.2116869119>.
- [50] I. Boettcher, A. V. Gorshkov, A. J. Kollár, J. Maciejko, S. Rayan, and R. Thomale, *Phys. Rev. B* **105**, 125118 (2022).
- [51] N. Cheng, F. Serafin, J. McInerney, Z. Rocklin, K. Sun, and X. Mao, *Phys. Rev. Lett.* **129**, 088002 (2022).
- [52] K. Ikeda, Y. Matsuki, and S. Aoki, *Canadian Journal of Physics* **101**, 630 (2023), <https://doi.org/10.1139/cjp-2022-0145>.
- [53] E. Kienzle and S. Rayan, *Advances in Mathematics* **409**, 108664 (2022).
- [54] P. M. Lenggenhager, J. Maciejko, and T. c. v. Bzdušek, *Phys. Rev. Lett.* **131**, 226401 (2023).
- [55] F. R. Lux and E. Prodan, *Phys. Rev. Lett.* **131**, 176603 (2023).
- [56] R. Mosseri and J. Vidal, *Phys. Rev. B* **108**, 035154 (2023).
- [57] N. Glusceovich, A. Samanta, S. Manna, and B. Roy, “Dynamic mass generation on two-dimensional electronic hyperbolic lattices,” (2023), [arXiv:2302.04864 \[cond-mat.str-el\]](https://arxiv.org/abs/2302.04864).
- [58] T. c. v. Bzdušek and J. Maciejko, *Phys. Rev. B* **106**, 155146 (2022).
- [59] R. Mosseri, R. Vogeler, and J. Vidal, *Phys. Rev. B* **106**, 155120 (2022).
- [60] H. Yuan, W. Zhang, Q. Pei, and X. Zhang, *Phys. Rev. B* **109**, L041109 (2024).
- [61] D.-H. Guan, L. Qi, Y. Zhou, A.-L. He, and Y.-F. Wang, unpublished.
- [62] J. B. Curtis, P. Narang, and V. Galitski, “Absence of weak localization on negative curvature surfaces,” (2023), [arXiv:2308.01351 \[cond-mat.dis-nn\]](https://arxiv.org/abs/2308.01351).
- [63] A. Chen, J. Maciejko, and I. Boettcher, “Anderson localization transition in disordered hyperbolic lattices,” (2023), [arXiv:2310.07978 \[cond-mat.dis-nn\]](https://arxiv.org/abs/2310.07978).
- [64] X. Zhu, J. Guo, N. P. Breuckmann, H. Guo, and S. Feng, *Journal of Physics: Condensed Matter* **33**, 335602 (2021).
- [65] P. Bienias, I. Boettcher, R. Belyansky, A. J. Kollár, and A. V. Gorshkov, *Phys. Rev. Lett.* **128**, 013601 (2022).
- [66] N. Glusceovich and B. Roy, “Magnetic catalysis in weakly interacting hyperbolic dirac materials,” (2023), [arXiv:2305.11174 \[cond-mat.str-el\]](https://arxiv.org/abs/2305.11174).
- [67] K. Ikeda, S. Aoki, and Y. Matsuki, *Journal of Physics: Condensed Matter* **33**, 485602 (2021).
- [68] S. Yu, X. Piao, and N. Park, *Phys. Rev. Lett.* **125**, 053901 (2020).
- [69] A. Stegmaier, L. K. Upreti, R. Thomale, and I. Boettcher, *Phys. Rev. Lett.* **128**, 166402 (2022).
- [70] D. M. Urwyler, P. M. Lenggenhager, I. Boettcher, R. Thomale, T. Neupert, and T. c. v. Bzdušek, *Phys. Rev. Lett.* **129**, 246402 (2022).
- [71] W. Zhang, H. Yuan, N. Sun, H. Sun, and X. Zhang, *Nature Communications* **13**, 2937 (2022).
- [72] Z.-R. Liu, C.-B. Hua, T. Peng, and B. Zhou, *Phys. Rev. B* **105**, 245301 (2022).
- [73] W. Zhang, F. Di, X. Zheng, H. Sun, and X. Zhang, *Nature Communications* **14**, 1083 (2023).
- [74] Z.-R. Liu, C.-B. Hua, T. Peng, R. Chen, and B. Zhou, *Phys. Rev. B* **107**, 125302 (2023).
- [75] Q. Pei, H. Yuan, W. Zhang, and X. Zhang, *Phys. Rev. B* **107**, 165145 (2023).
- [76] Y.-L. Tao and Y. Xu, *Phys. Rev. B* **107**, 184201 (2023).
- [77] T. Tummuru, A. Chen, P. M. Lenggenhager, T. Neupert, J. Maciejko, and T. c. v. Bzdušek, *Phys. Rev. Lett.* **132**, 206601 (2024).
- [78] A. Chen, Y. Guan, P. M. Lenggenhager, J. Maciejko, I. Boettcher, and T. c. v. Bzdušek, *Phys. Rev. B* **108**, 085114 (2023).
- [79] J. Sun, C.-A. Li, S. Feng, and H. Guo, *Phys. Rev. B* **108**, 075122 (2023).
- [80] P. Basteiro, F. Dusel, J. Erdmenger, D. Herdt, H. Hinrichsen, R. Meyer, and M. Schrauth, *Phys. Rev. Lett.* **130**, 091604 (2023).
- [81] A. J. Kollár, M. Fitzpatrick, and A. A. Houck, *Nature* **571**, 45 (2019).
- [82] P. M. Lenggenhager, A. Stegmaier, L. K. Upreti, T. Hofmann, T. Helbig, A. Vollhardt, M. Greiter, C. H. Lee, S. Imhof, H. Brand, T. Kießling, I. Boettcher, T. Neupert, R. Thomale, and T. Bzdušek, *Nature Communications* **13**, 4373 (2022).
- [83] A. Chen, H. Brand, T. Helbig, T. Hofmann, S. Imhof, A. Fritzsche, T. Kießling, A. Stegmaier, L. K. Upreti, T. Neupert, T. Bzdušek, M. Greiter, R. Thomale, and I. Boettcher, *Nature Communications* **14**, 622 (2023).
- [84] See Supplemental Material for details on single-particle states and FCIs in the octagon-kagome and nonagon-

kagome lattice models.

- [85] J. A. Kjäll and J. E. Moore, *Phys. Rev. B* **85**, 235137 (2012).
- [86] Notice that $|101010\rangle_{\text{TFB}}$ is not equal to $|101010\rangle_{\text{FCI}}$ and the latter one denotes the GS of $\nu = 1/2$ FCI.
- [87] F. D. M. Haldane, *Phys. Rev. Lett.* **107**, 116801 (2011).
- [88] K. Yang, *Phys. Rev. B* **88**, 241105 (2013).
- [89] T. Can, M. Laskin, and P. Wiegmann, *Phys. Rev. Lett.* **113**, 046803 (2014).
- [90] T. Can, M. Laskin, and P. B. Wiegmann, *Annals of Physics* **362**, 752 (2015).
- [91] K. Yang, *Phys. Rev. B* **93**, 161302 (2016).
- [92] T. Can, Y. H. Chiu, M. Laskin, and P. Wiegmann, *Phys. Rev. Lett.* **117**, 266803 (2016).
- [93] Y.-H. Wu, H.-H. Tu, and G. J. Sreejith, *Phys. Rev. A* **96**, 033622 (2017).
- [94] S.-F. Liou, F. D. M. Haldane, K. Yang, and E. H. Rezayi, *Phys. Rev. Lett.* **123**, 146801 (2019).